Available online at www.sciencedirect.com
SCIENCE DIRECT®
Polymer 44 (2003) 4949–4958
polymer
www.elsevier.com/locate/polymer

Synthesis and characterisation of a nematic homo-polyurethane

Domenico Acierno[a], Eugenio Amendola[b], Cosimo Carfagna[a], Simona Concilio[c], Pio Iannelli[c,*], Loredana Incarnato[c], Paola Scarfato[a]

[a]*Dipartimento di Ingegneria dei Materiali e della Produzione, Università di Napoli, P.le Tecchio, I-80125 Napoli, Italy*
[b]*Istituto per la Tecnologia dei Materiali Compositi-CNR, P.le Tecchio, I-80125 Napoli, Italy*
[c]*Dipartimento di Ingegneria Chimica ed Alimentare, Università di Salerno, via Ponte Don Melillo, I-84084 Fisciano (Salerno), Italy*

Received 25 May 2003; received in revised form 28 May 2003; accepted 30 May 2003

Abstract

The presence of hydrogen bonds in the chemical structure of polymers promotes and stabilises the crystalline phase. For liquid crystalline (LC) polymers, the side insertion of aliphatic units to the mesogenic unit is a suitable artifice to decrease the crystalline stability, without significantly affecting the stability of the LC phases. Here, we report on the synthesis of a LC homo-polyurethane with high hydrogen bond concentration along the chain and bearing an *n*-pentyl side-chain. Rheological behaviour, thermal analysis, and X-ray diffraction show that the stable LC phase is the nematic.

Keywords: Polyurethane; Nematic phase; Rheology

1. Introduction

Liquid crystalline (LC) systems have been studied extensively for their interesting properties and the related technological applications. Three decades ago, when first reports were published [1–3], a large number of polymeric systems showing the liquid crystalline order (PLCs) were synthesised and characterised. It was soon clear that the main ingredients to prepare PCLs are molecular segments with elongated shape and rigid conformation. Mesogenic activity may be quantified by using the *axial ratio*, defined as the ratio between the length of a rigid molecular segment (with no or with reduced conformational degree of freedom) and its transversal thickness. The higher is the *axial ratio*, the higher will be the mesogenic character of that molecular segment.

Depending on the insertion of mesogenic unit along the chain or attached to the chain, two classes of PCLs are established: the *main-chain* and the *side-chain* type PCLs. Usually, the presence of strong polar groups in the chain should be avoided because, whilst they stabilize the mesogen-to-mesogen interaction and the LC order, they may induce crystallisation, too. In this case, the large temperature range of stability of the crystalline phase hampers LC phases.

Among PCLs, only few examples of LC polyurethanes (PUCLs) are known. In fact, hydrogen bond is particular effective in improving transversal register between adjacent chains, acting as a reversible inter-chain locking. Accordingly, when LC phases are observed they are usually of ordered smectic type [4–7], whilst only few examples of nematic PUCLs copolymers, block copolymers or polymers with a low concentration of hydrogen bonds in the chain have been reported [8–10].

Here, we report on the synthesis and the characterisation of a homo-polymer PUCL having formula:

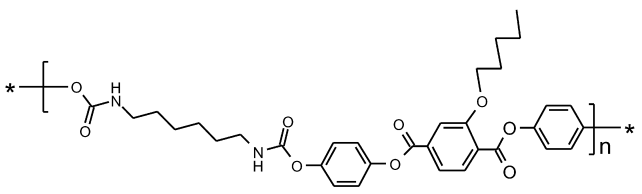

T5

The insertion of a pendant flexible group to the chain is a way to reduce crystalline stability, by decreasing

* Corresponding author. Fax: +39-089-964-057.
E-mail address: iannelli@dica.unisa.it (P. Iannelli).

0032-3861/03/$ - see front matter © 2003 Elsevier Ltd. All rights reserved.
doi:10.1016/S0032-3861(03)00488-9

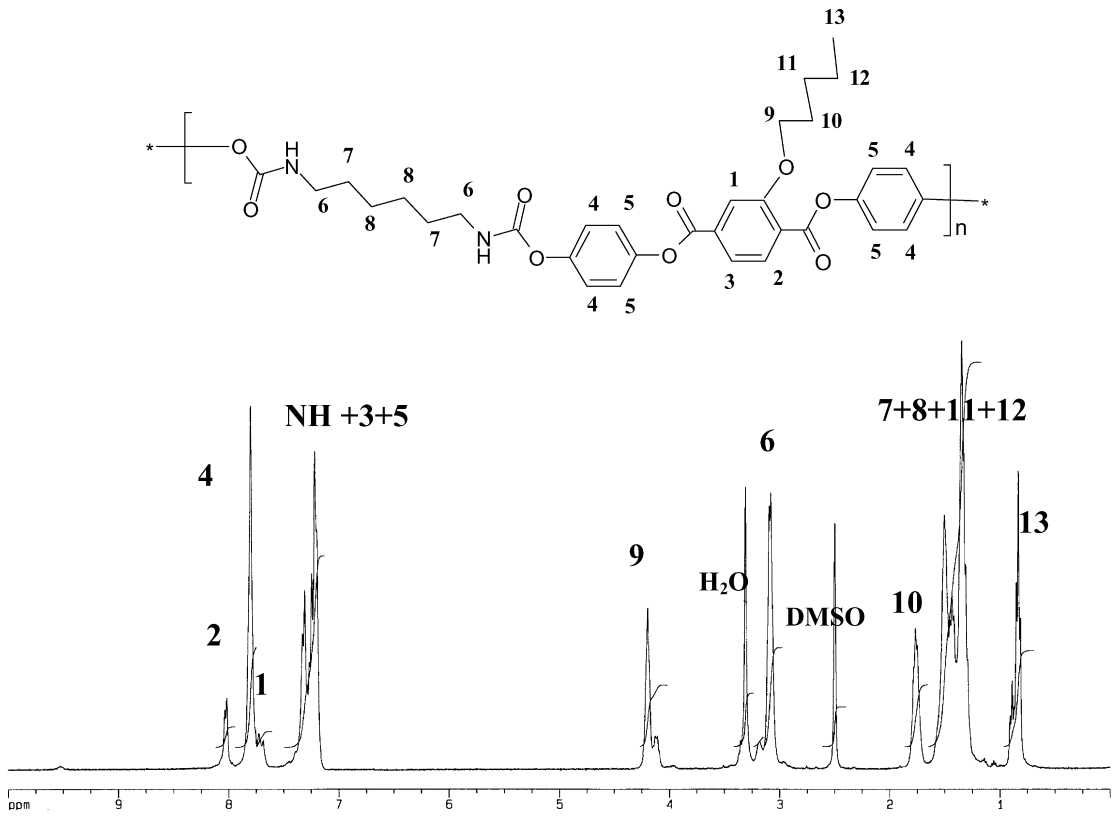

Fig. 1. ^{1}H NMR spectra of **T5** (DMSO-d_6 as solvent).

chain-to-chain register but without significantly affecting the LC order [11–18]. In the case of **T5**, the side group competes with hydrogen bond: the result is the appearing of the less structured and fluid nematic phase.

2. Experimental

2.1. Materials

All reagents and solvents were purchased from Aldrich and Carlo Erba. They were used without further purification. Hydroxyterephthalic acid and *n*-pentyloxyterephthalic acids were synthesized according to previously reported procedures [17,18].

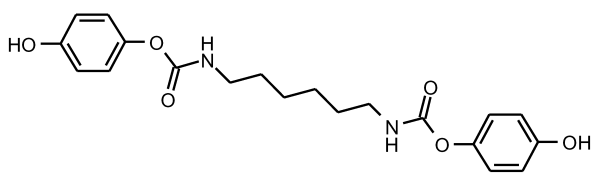

1

Twenty grams of hydroquinone (0.1816 mol) are dissolved into 30.0 ml of *N*,*N*-dimethylformamide (DMF). 3.81 g of diisocyanate hexane are added (0.02270 mol) and the solution is stirred at 80 °C under argon for six hours with a catalytic amount of $SnCl_2$. At the end, the solution is poured in 500 ml of water and moderately heated for 10 min in order to coagulate the solid. After cooling at room temperature, the suspension is placed in a refrigerator for two hours. The solid is collected by filtration and washed with water directly on the filter, and then it is treated with 200 ml of boiling ethanol. When cooled at room temperature, the solution is filtered to remove the colloidal suspension, placed in refrigerator overnight, and filtered once more. Adding 400 ml of water precipitates fine white solid. After cooling for one hour in a refrigerator, the solid is collected by fast filtration. The white solid **1** is dried in an oven at 60 °C under vacuum.

Yield ≈ 65%. $T_m = 181.7$ °C, $\Delta H_m = 141.4$ J/g. The proton resonance data are in agreement with the expected values (DMSO-d_6): δ (ppm) = 7.57 (t, 2H); 6.86 (d, 4H); 6.71 (d, 4H); 3.02 (m, 4H); 1.44 (m, 4H); 1.30 (m, 4H).

2.1.1. Polymer synthesis

T5 is synthesised by interfacial polycondensation reaction of **1** and pentyloxytherephtaloyl chloride (**2**). Approx. 1.5 g of **1** is dissolved in 100 ml of water with stoichiometric amount of KOH and 0.700 g of benzyltriethylammonium chloride as surfactant. The equimolar amount of **2** is dissolved in 50 cc of chloroform. The two solutions are vigorously stirred in a blender for 12 min. The polymer is precipitated by addition of *n*-heptane (100 ml) and, after filtration, washed once with a chloroform/heptane solution

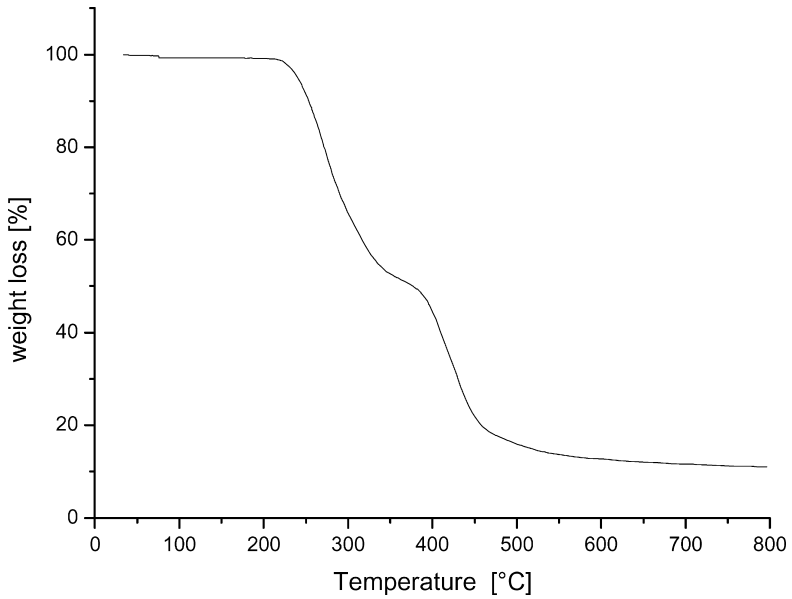

Fig. 2. Thermogravimetric curve of **T5** taken under nitrogen atmosphere at 10 °C/min.

(30/70 v/v), once with ethanol, three times with water, and, finally, washed once more with ethanol. Then, the polymer is placed to extract with boiling methanol in a Soxhlet apparatus for one day, and dried at 60 °C under vacuum. After a recrystallisation from chloroform–heptane, **T5** is recovered as a white soft powder. The proton resonance data are in agreement with the expected values (DMSO-d_6): δ (ppm) = 8.00 (d, 1H); 7.79 (m, 4H); 7.31–7.21 (m, 8H); 4.19 (t, 2H); 3.08 (m, 4H); 1.75 (m, 2H); 1.50–1.37 (m, 12H); 0.83 (m, 3H). The ^{1}H NMR spectra is shown in Fig. 1.

2.2. Characterisation

Fibres were extruded from the nematic phase and cooled down to room temperature. The average diameter of fibres is 200–300 μm.

Thermal measurements were performed by a DSC-7 Perkin Elmer calorimeter under nitrogen flow at 10 °C/min rate.

Thermogravimetric analysis was performed by a Mettler TGA apparatus at 10 °C/min under nitrogen flow.

Polarised optical microscopy was performed by a Jenapol microscope fitted with a Linkam THMS 600 hot stage.

X-ray diffraction spectra were recorded using a flat camera with a sample-to-film distance of 90.0 mm (Ni-filtered Cu Kα radiation). High temperature X-ray diffraction patterns were collected using a modified Linkam THMS 600 hot stage. The Fujifilm MS 2025 imaging plate and a Fuji Bio-imaging Analyzer System, mod. BAS-1800, were used for recording and digitising the diffraction patterns.

^{1}H NMR spectra were recorded with a Brucker DRX/400 Spectrometer. Chemical shifts are reported relative to the residual solvent peak (dimethylsulfoxide-d6).

Solution viscosity measurements (Ubbelohde viscometer) were performed in *N*-methylpirrolidinone at 25.0 °C. A M2000 Spectrometer (by Midac Co.) was adopted to collect IR spectra.

Dynamic mechanical tensile analysis was carried out by means of a Perkin Elmer DMA 7 analyser, in the temperature range between 20 and 150 °C at 5 °C/min heating rate under nitrogen flow. Fibre length was approximately 15 mm and diameter was 300 μm. Frequency was set at 1 Hz, with dynamical load ranging from 10 to 210 mN.

Small-amplitude oscillatory measurements were performed on an ARES rheometer (Rheometrics, Inc.) having parallel plates geometry, with a plate radius of 12.5 mm and a gap of 0.5 mm after thermal adjustment. The material was tested as powder specimens, after drying at 75 °C in a vacuum oven for 4 h. Before starting the tests, the powder samples of polymer were loaded into the rheometer at 190 °C (isotropic state), held at this temperature for 10 min in order to erase the previous thermo-mechanical history and destroy the crystalline phase, then cooled to the measuring temperature with a rate of 20 °C/min. Temperature sweep tests were carried out in dynamic regime at frequency of $\omega = 5$ rad/s and in the temperature range of 160–80 °C (cooling mode, at rate of 10 °C/min). Dynamic frequency sweep tests were performed in the frequency range of $\omega = 0.1 \div 100$ rad/s at $T = 150$ °C, 130 °C (in the isotropic phase), and $T =$ 90 °C (in the nematic phase). All rheological tests were conducted at constant strain amplitude of 5%, proven to be in the linear viscoelastic region of the polymer, using nitrogen atmosphere, in order to minimise thermo-oxidative degradation phenomena.

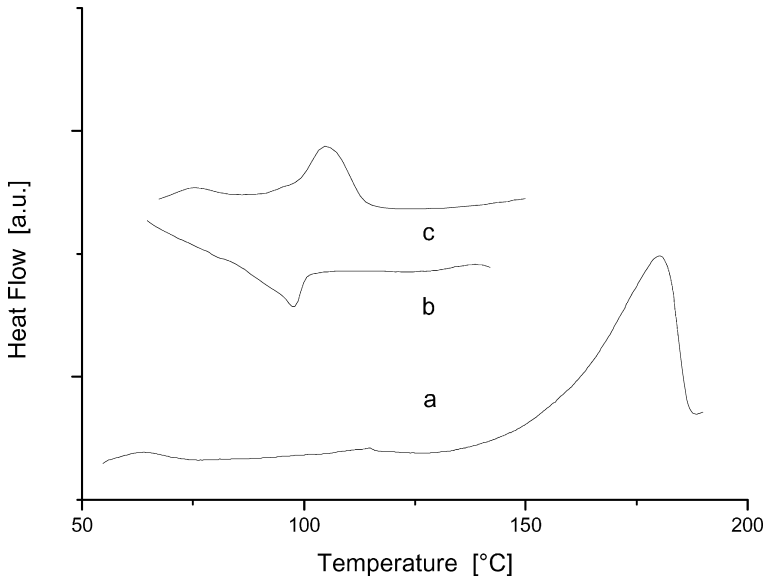

Fig. 3. Calorimetric traces of **T5**: (a) first heating run, showing the melting transition; (b) first cooling run, showing the anisotropization transition; (c) second heating run, showing the isotropization transition.

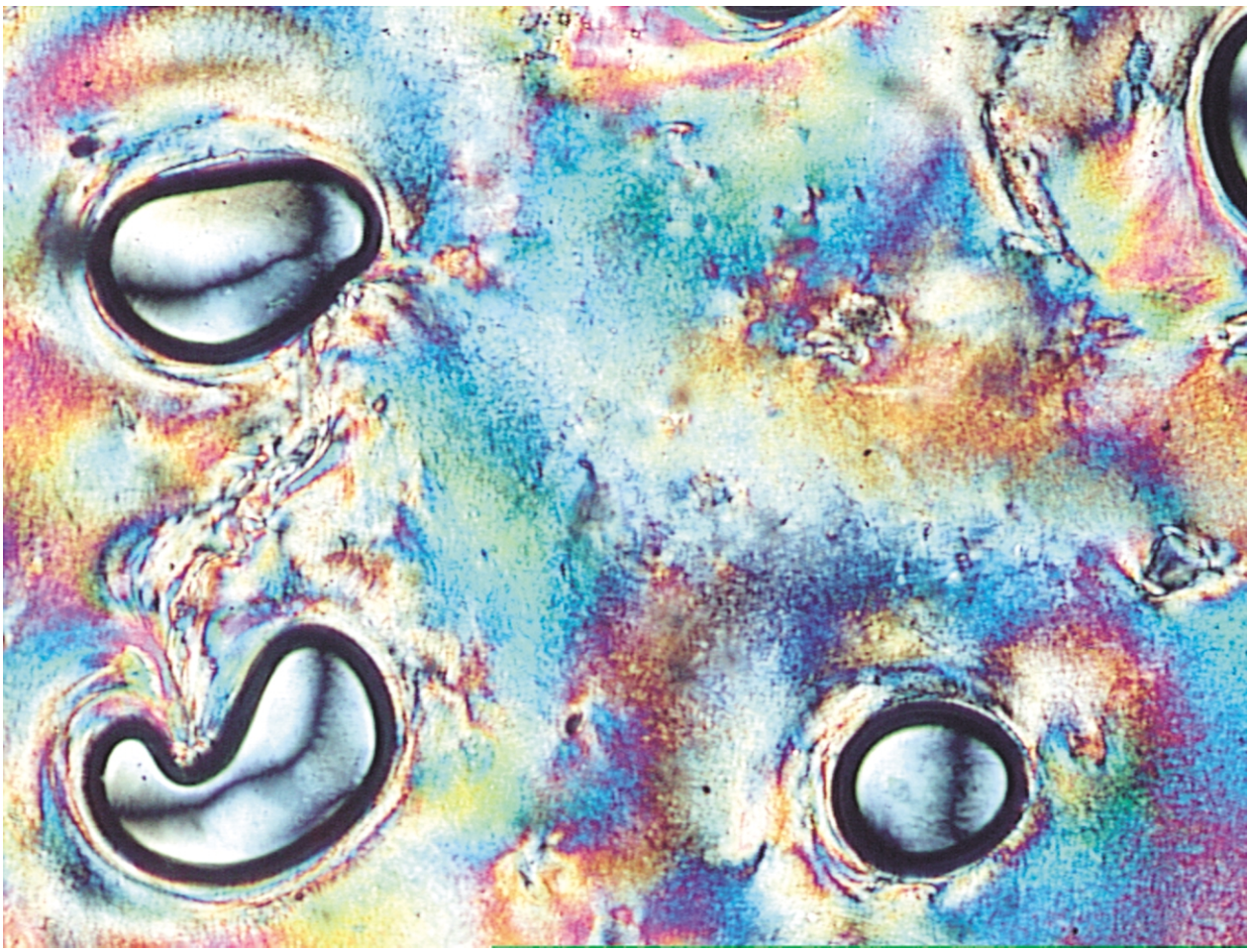

Fig. 4. Optical texture of **T5**, taken at about 100 °C during cooling run. Crossed polarisers, × 100.

3. Results and discussion

3.1. Synthesis

Isocyanate easily reacts with nucleofilic agents giving rise to numerous products. The most important are urethanes, which are obtained by reaction of isocyanate with alcohols. Tin compounds catalyse this reaction, increasing the kinetic by a factor of 10^4–10^5 and making urethane synthesis very fast and suitable for large-scale production. Reagents must be perfectly dry in order to avoid the quick reaction of water with urethanes and isocyanates bringing to branching or crosslinking. In the case of **T5** we avoid this problem by preparing monomer **1** first, which has two urethane linkages, then making interfacial polycondensation reaction of **1** with the alkoxyterephthaloyl chloride. The yield is 60% and the inherent viscosity is $\eta_{inh} = 0.62$ dl/g with polymer concentration of 0.20 g/dl.

Thermal stability is good at temperature lower than 200 °C, with 5% degradation occurring at 230 °C (Fig. 2).

3.2. Phase behaviour

Calorimetric runs, made on virgin samples of **T5**, are shown in Fig. 3. Virgin polymer is semi-crystalline material which melts to a viscous isotropic fluid at $T_m = 173.3$ °C with a broad endothermic transition (melting enthalpy $\Delta H_m = 18.6$ J/g, Fig. 3(a)). If the sample is annealed in the isotropic phase for at least 10 min; crystallisation does not take place in the subsequent cooling run and only a weak and broad exothermic transition is observed, peaked at 98 °C ($\Delta H_{an=}$1.5 J/g, Fig. 3(b)). This transition is reversible according to the second heating run, which shows a broad endothermic transition at 105 °C (Fig. 3(c)). By optical analysis, the two transitions correspond, respectively, to the anisotropization and to the isotropization of the viscous fluid. Optical texture, taken at about 100 °C during cooling (Fig. 4), and the fluid nature of the anisotropic phase are consistent with the nematic character of the phase. No crystallisation process is observed during successive heating and cooling runs. Crystallinity is only recovered after annealing at temperature higher than the glassy temperature ($T_g = 68$ °C, evaluated by DMTA measurements).

X-ray diffraction patterns of both virgin and molten sample of **T5**, taken at room temperature, are given in Fig. 5. For virgin **T5** sample, the X-ray pattern in Fig. 5(a) shows the mesophase nature of the material. The nematic nature of the phase quenched from the molten anisotropic state is clearly shown in Fig. 5(b): only a diffuse halo is visible, compatible with the nematic phase (halo peaked at $(sin\theta)/\lambda = 0.11$ Å^{-1} and no Bragg diffraction for lattice distances lower than about 41 Å).

Fibre samples (Fig. 6(a)) retain the nematic structure at room temperature and crystallisation is induced only by annealing at 100 °C for 1 h (Fig. 6(b)). The diffraction ring

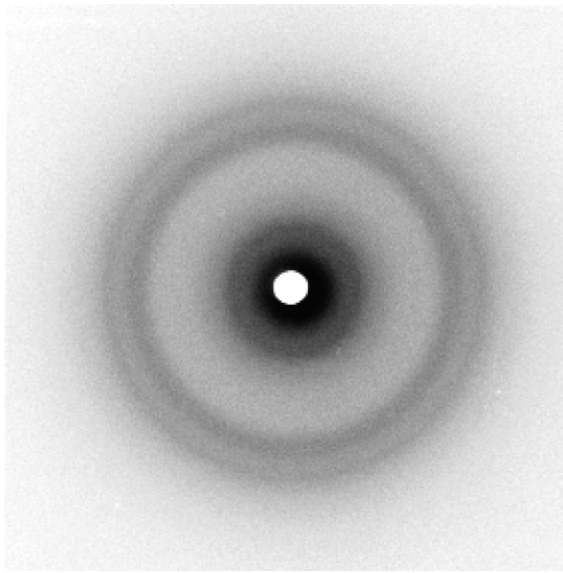

a

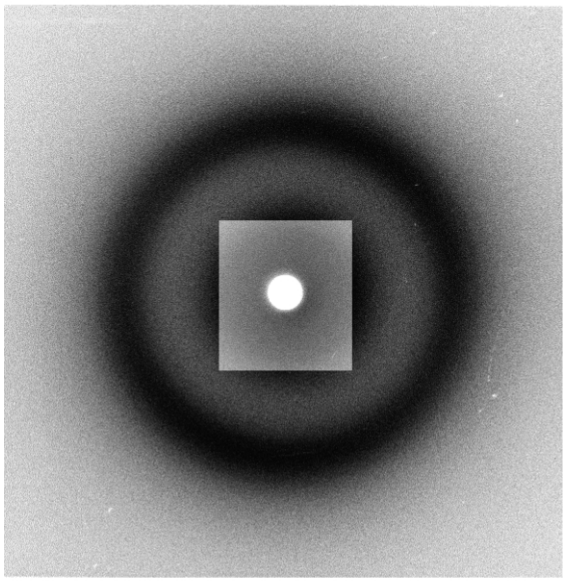

b

Fig. 5. X-ray diffraction patterns of **T5**: (a) virgin powder sample-crystalline phase; (b) molten sample-nematic phase.

at lower angle corresponds to a *d*-spacing of 21.1 Å, which may be accounted for by the inter-chain distances, in the hypothesis of a supramolecular type packing of chains similar to that observed for analogous side attached PLCs [17]. This hypothesis is in agreement with the equatorial nature of the low angle reflection. Moreover, meridian and out-meridian reflections are not detectable, suggesting the absence of chain-to-chain transversal correlation.

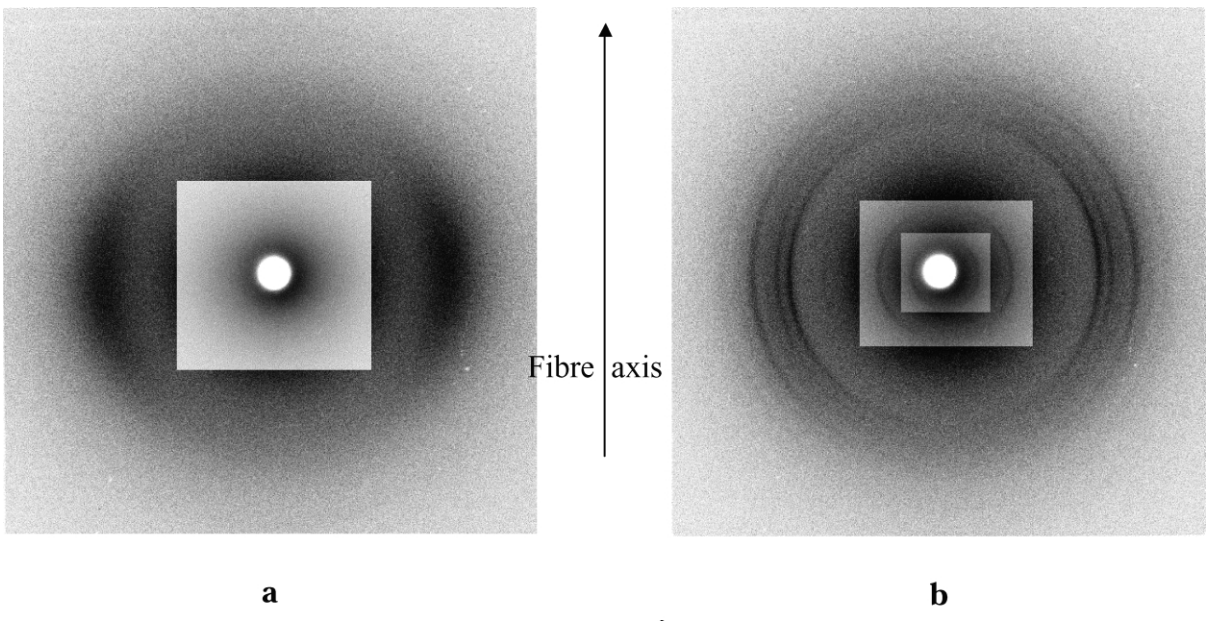

Fig. 6. X-ray diffraction patterns of fibre sample of **T5**: (a) virgin fibre-nematic phase; (b) annealed fibre, 1 h at 100 °C—crystalline phase.

3.3. IR spectroscopy

The room temperature IR spectrum of a virgin sample of **T5** is given in Figs. 7 and 8. The N–H stretching absorption band is characterised by two overlapped signals centred at 3394 and 3324 cm^{-1}. According to Hong et al. [10], they correspond to the stretching of N–H bond, free or hydrogen bonded, respectively. Similarly, the strong C=O stretching absorption band is expected to be the sum of several signals due to the two different carbonyl units (esteric and urethanic carbonyl), and the occurrence or not of hydrogen bonding. In our case, this signal shows only two overlapped peaks centred at 1745 and 1719 cm^{-1}, assigned to the free and the hydrogen bonded carbonyl units, respectively (a small shoulder is detectable at 1699 cm^{-1}, but the signal is weak).

In the case of a virgin sample heated upon the melt at 190 °C and then quickly quenched at room temperature, the N–H and C=O absorption bands at lower frequency clearly decrease (Fig. 9), according to the partial disruption of the hydrogen bond network. When thermal treatment includes also an annealing at high temperature (i.e. 160–170 °C for 30 min) in the liquid isotropic state, the IR spectrum is identical to the previous one showing that the hydrogen bond network collapses quickly in the isotropic liquid phase. This is quite in contrast with the inhibition effect that annealing in the isotropic liquid phase has on crystallisation process of **T5**, as discussed in the phase behaviour section. Probably a long annealing in the isotropic liquid phase might increase the distance between N–H and C=O units due to the relatively good mobility of macromolecules. Then, when sample is cooled, the original hydrogen bond network and the related ordered packing of macromolecules could be restored only after a prolonged re-annealing.

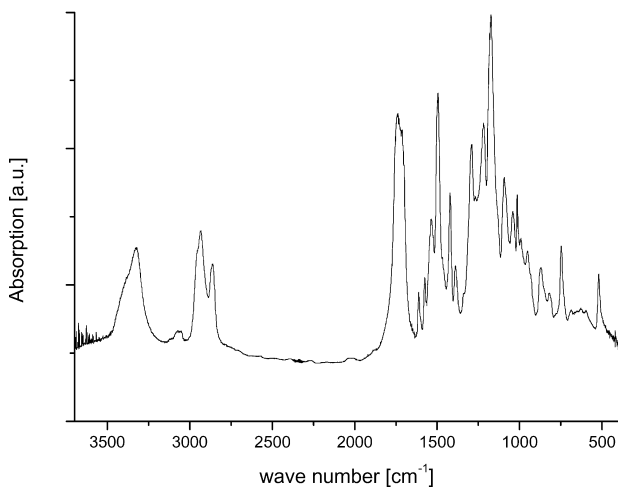

Fig. 7. IR spectra of **T5**, taken at room temperature on virgin sample.

3.4. Rheology

Rheological measurements were performed to further understand the phase behaviour of **T5**, being the viscoelastic response highly sensitive to meso-scale structure of liquid-crystalline polymer systems [19]. In particular, temperature sweep tests in dynamic regime represent a valid tool to detect isotropic/nematic transition [20]. The temperature dependence of the complex viscosity (η^*) is reported in Fig. 10, where the calorimetric data are also shown for comparison. Examination of graph reveals that η^* monotonically increases with decreasing the temperature, nevertheless a gradual rheological transition, with a reduced temperature dependence of the complex viscosity, takes place in the same temperature range in which thermal events associated with the anisotropization occur. Then, the appearance of a plateau in the η^* curve in the temperature

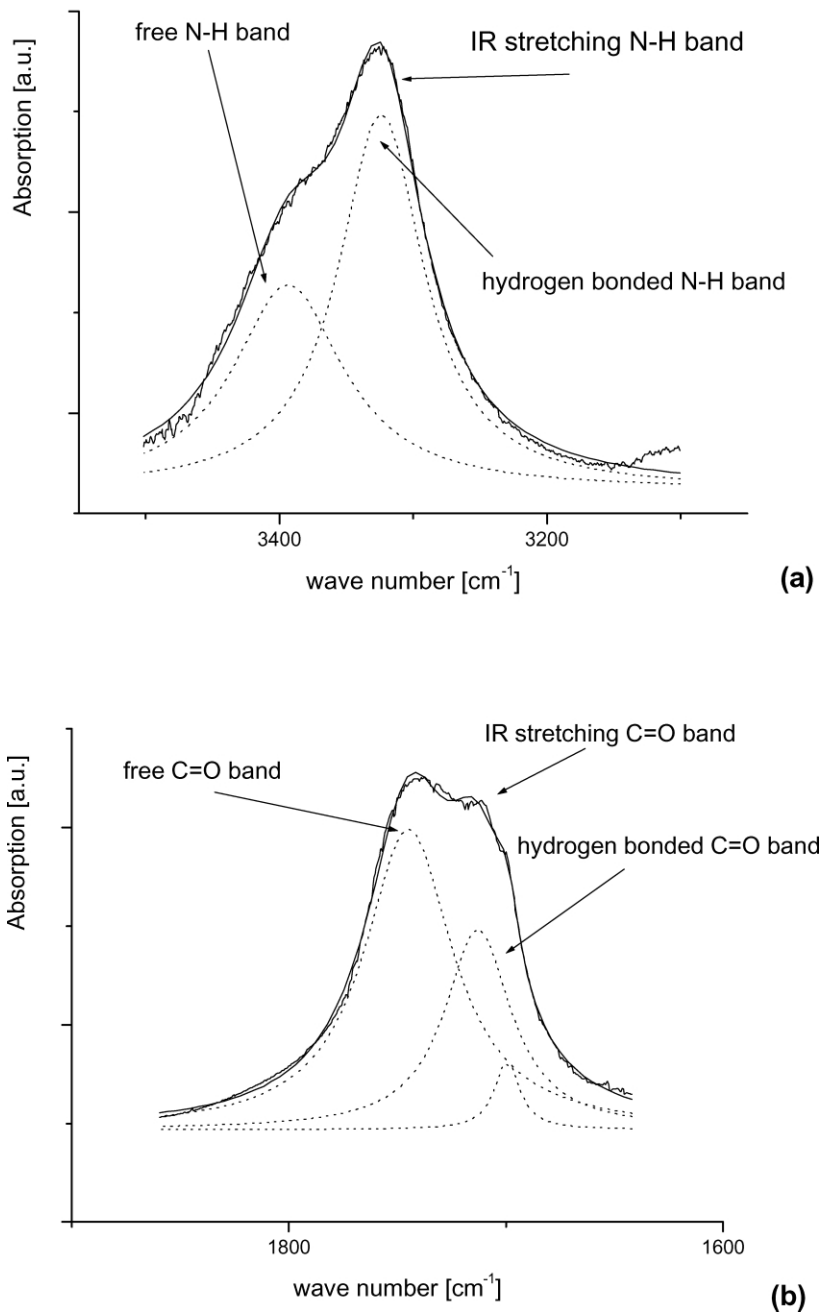

Fig. 8. Deconvolution of N–H (a) and C=O; (b) stretching IR absorption bands (data taken from IR spectra given in Fig. 7—see text).

range of 110–90 °C can be attributed to the broad isotropic-nematic transition. The absence of the typical drop in the η^* curve corresponding to this transition could be explained hypothesising that, at decreasing temperatures, the reorganization of inter-molecular hydrogen bonds competes with the anisotropization [21]. Consequently, the complex viscosity trend can be a compromise between these two phenomena, whose effects on η^* are opposed. Another possible explanation for the observed plateau takes into account that the drop in the viscosity at the isotropization temperature in liquid-crystalline polymers is not a general behaviour and seems to depend on the shear rate regime at which the viscosity is measured [22–23]. In our case, the viscosity values are measured performing dynamic and not steady shear experiments, where higher degrees of orientation (and then lower viscosities) may be achieved. For several TLCPs the general shape of the flow curve is the same in dynamic and steady flow measurements, also if the Cox–Mertz rule is usually not satisfied quantitatively. Nevertheless, dynamic tests still represent a valid tool for comparative measurements to detect transitions.

In order to investigate the frequency dependence of

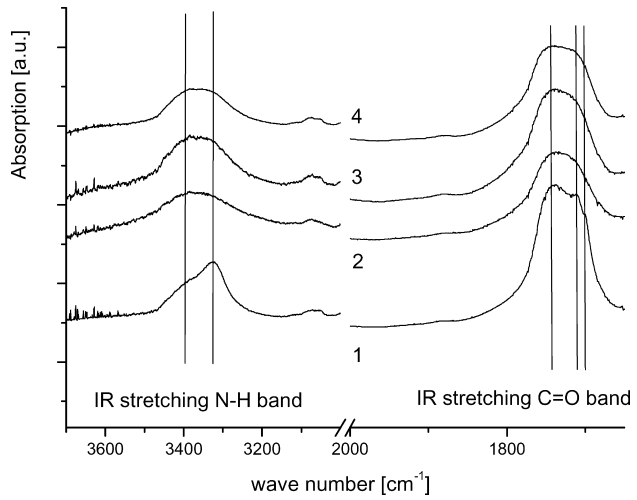

Fig. 9. IR spectra of **T5**, taken at room temperature on samples treated in different conditions: (1) virgin sample; (2) quenched sample from the isotropic phase (190 °C); (3) previous sample annealed 30 min at 170 °C; (4) fibre sample.

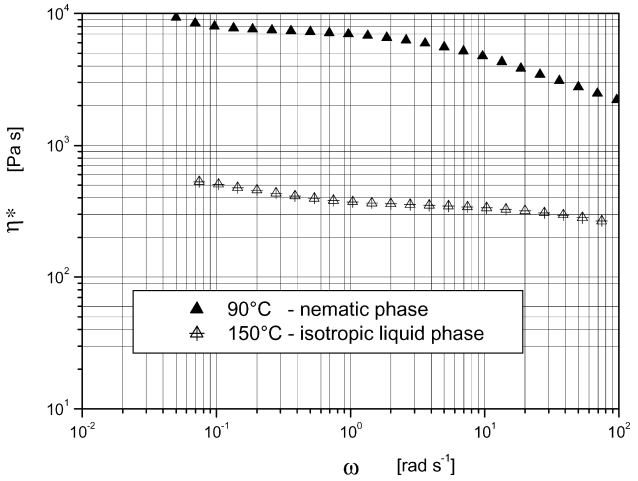

Fig. 11. Complex viscosity η^* versus frequency. Tests were performed with constant strain at 5%, in the isotropic ($T = 150$ °C) and nematic phase (90 °C).

viscoelastic response of **T5** in the isotropic liquid phase and in the nematic one, frequency sweep tests were performed at 150 and 90 °C, respectively. The complex viscosity profiles obtained are compared in Fig. 11.

The $\eta^*(\omega)$ curve determined at 90 °C has a three region shape, similar to the steady flow response of a nematic polymer melt [24]: the low and high frequency regions ($\omega <$ 0.2 rad/s and $\omega >$ 1.5 rad/s), in which a shear thinning trend can be observed, and the region with $\omega = 0.2 \div 1.5$ rad/s, in which the flow curve exhibits a quasi-Newtonian plateau. The $\eta^*(\omega)$ curve measured at 150 °C shows a similar feature, with a shear thinning trend at low frequency ($\omega <$ 1 rad/s), a quasi-Newtonian plateau in the frequency range of $\omega = 1 \div 10$ rad/s and a new moderate shear thinning trend for $\omega >$ 10 rad/s. These last two zones are commonly observed for many isotropic polymer melts, whereas the first one is unusual and may be explained with the occurrence of an extended hydrogen bond network, as found also for other polyurethane-based systems [21,25–28]. In fact, the extensive inter-molecular hydrogen bonding restricts the mobility of **T5** chains. Consequently, in the isotropic phase a liquid–liquid microphase separation may exist at low ω ($\omega <$ 1 rad/s) [26], which becomes gradually broken by increasing the oscillation frequency.

The dynamic storage (G') and loss (G'') moduli measured in the isotropic and nematic phases are reported in Fig. 12 as a function of oscillation frequency. In both phases G' and G'' increase monotonically with the viscous response dominating on the elastic one in the whole frequency range examined. Moreover, comparing the G' curves, which are very sensitive to morphological state of the sample, it comes out that the storage modulus shows more marked frequency dependence in the isotropic phase than in the

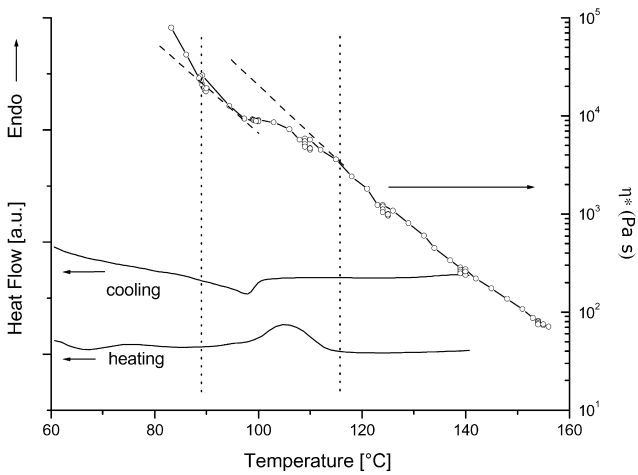

Fig. 10. Complex viscosity η^* versus temperature is compared to the calorimetric data of **T5**. Cooling and heating scans at 10 °C/min; constant frequency ω at 5 rad/s and constant strain at 5%.

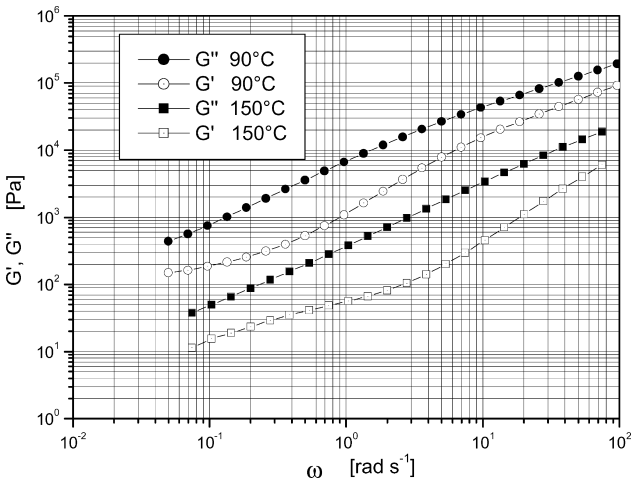

Fig. 12. G' and G'' moduli versus frequency. Tests were performed with constant strain at 5%, in the isotropic ($T = 150$ °C) and nematic phase (90 °C).

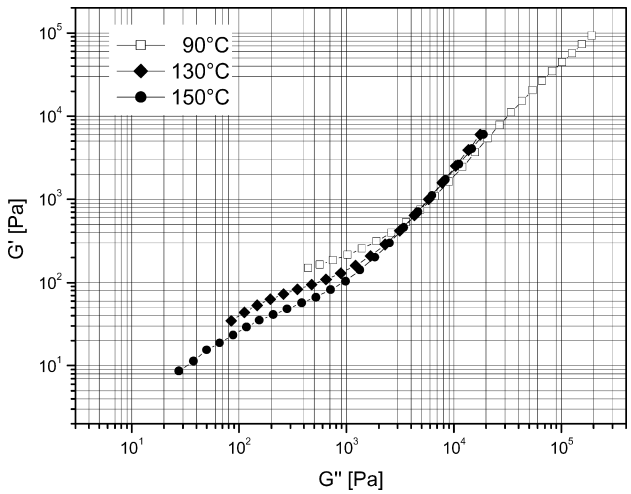

Fig. 13. log G' versus log G'' plots (Han plots) at 90, 130, and 150 °C. Tests were performed with constant strain at 5%, in the frequency range of $\omega = 0.1 \div 100$ rad/s.

nematic one. This result suggests that a higher degree of order exists at 90 °C than at 150 °C. However, both the storage and loss moduli do not show the characteristic terminal flow behaviour of polymer melts, at any of the temperatures investigated. The absence of the terminal regime for **T5** is not clear, but it could be attributed to the effect of a large-scale defect structure, as suggested by some authors and reported in literature for other thermotropic systems [29–32].

Fig. 13 shows log G' versus log G'' plots, referred to as Han plots [33], determined at 150 and 90 °C, to better evidence the temperature dependence of **T5** morphology. It is well known, in fact, that a different temperature independent Han plot is obtained for each homogeneous polymer phase [34]. The graph points out that during cooling from 150 to 90 °C the Han plot moves upward and merges into a single curve with a slope in the terminal region becoming smaller with decreasing temperature. This temperature dependence of the Han plot is further evidence that the morphology of **T5** varies with the temperature, although the plot cannot determine how the morphology changes [21].

4. Conclusions

Homo-polyurethanes are crystalline materials due to the strong hydrogen bond network and only few examples of homo-PUCLs showing a smectic phase have been reported in literature. The nematic phase has been observed only in the case of copolymers with low hydrogen bond concentration, or block copolymers with alternating LC and urethane sequences. We have synthesised the homopolymer **T5**, in which the side chain flexible aliphatic group destabilises the crystalline phase, despite the high urethane units' density and the structural order along the chain. In conclusion, we found that the side group insertion is an efficient synthetic tool for preparing nematic polyurethanes.

Acknowledgements

Support by Ministero dell'Istruzione, dell'Università e della Ricerca (MIUR) in financing this research project is acknowledged (PRIN 2001-'Adesivi gommosi su base cristallo liquida').

References

[1] Kwolek SL. US Patent 3,671,542 (Dupont Co.); 1972.
[2] Roviello A, Sirigu A. Gazz Chimi Italiana 1977;107:333.
[3] de Gennes PG. C R Hebd Seances Acada Sci, Ser B 1975;282:101.
[4] Papadimitrakopoulos F, Sawa E, MacKnight W. Macromolecules 1992;25:4671.
[5] Papadimitrakopoulos F, Sawa E, MacKnight W. Macromolecules 1992;25:4682.
[6] Tang W, Farris RJ, MacKnight WJ, Eisenbach CD. Macromolecules 1994;27:2814.
[7] Padmavathy T, Srinivasan KSV. J Polym Sci, Polym Chem 2002;40:1527.
[8] Angeloni AS, Laus M, Chiellini E, Galli G, Francescangeli O. Eur Polym J 1995;31:253.
[9] Francescangeli O, Yang B, Laus M, Angeloni AS, Galli G, Chiellini E. J Polym Sci, Polym Phys 1995;33:699.
[10] Yen FS, Lin LL, Hong JL. Macromolecules 1999;32:3068.
[11] Ballauff M, Schmidt GM. Makromol Chem, Rapid Commun 1987;8:93.
[12] Rodriguez-Parada JM, Duran R, Wegner G. Macromolecules 1989;22:2507.
[13] Kricheldorf HR, Engelhardt J. Makromol Chem 1990;191:2017.
[14] Stern R, Ballauff M, Lieser G, Wegner G. Polymer 1991;32:2096.
[15] Harkness BR, Watanabe J. Macromolecules 1991;24:6759.
[16] Watanabe J, Harkness BR, Sone M. Polym J 1992;24:1119.
[17] Caruso U, Pragliola S, Roviello A, Sirigu A, Iannelli P. Macromolecules 1995;28:6089.
[18] Iannelli P, Pragliola S, Roviello A, Sirigu A. Macromolecules 1997;30:4247.
[19] Dealy JM, Wissbrum KF. Melt rheology and its role in plastics processing. Dordrecht: Kluwer Academic Publishers; 1999.
[20] Cogswell FN, Wissbrun KF. Rheology and processing of liquid crystal polymer melts. In: Acierno D, Collyer AA, editors. Rheology and processing of liquid crystal polymers. London: Chapman and Hall; 1996. p. 86–121.
[21] Yoon PJ, Han CD. Macromolecules 2000;33:2171.
[22] Stenhouse PJ, Valles EM, Kantor SW, MacKnight WJ. Macromolecules 1989;22:1467.
[23] Wissbrun KF, Griffin AC. J Polym Sci, Polym Phys Ed 1982;20:1835.
[24] Onogi S, Asada T. Rheology and rheo-optics of polymer liquid crystals. In: Astarita G, Marrucci G, Nicolais L, editors. Rheology, vol. 1. New York: Plenum Press; 1980. p. 127–47.
[25] Papadimitrakopoulos F, Kantor SW, MacKnight WJ. Polym Preprints 1990;31:486.
[26] Tang W, MacKnight WJ, Hsu SL. Macromolecules 1995;28:4284.
[27] Jaúregui-Beloqui B, Fernández-García JC, Orgilés-Barceló AC, Mahiques-Bujanda MM, Martín-Martínez JM. Int J Adhesion and Adhesives 1999;19:321.

[28] Torró-Palau AM, Fernández-García JC, Orgilés-Barceló AC, Martín-Martínez JM. Int J Adhesion and Adhesives 2001;21:1.
[29] Gillmor JR, Colby RH, Hall E, Ober CK. J Rheol 1994;38:1623.
[30] Zhou WJ, Kornfield JA, Ugaz VM, Burghardt WR, Link DR, Clark NA. Macromolecules 1999;32:5581.
[31] Kim SS, Han CD. Macromolecules 1993;26:6633.
[32] Driscoll P, Masuda T, Fujiwara K. Macromolecules 1991;24:1567.
[33] Neumann C, Loveday DR, Abetz V, Stadler R. Macromolecules 1998; 31:2493.
[34] Han CD, Kim JK. Macromolecules 1989;22:4292.